Journal of Mathematical Chemistry, Vol. 39, No. 1, January 2006 (© 2005)
DOI: 10.1007/s10910-005-9009-1

Ionization of 1-D model atom in an intense laser field based on asymptotic boundary conditions and symplectic algorithm

Yue-Ying Qi*

School of Electrical Engineering, Jiaxing University, Jiaxing 314001, People's Republic of China
Institute of Atomic and Molecular Physics, Jilin University, Changchun 130012, People's Republic of China
E-mail: qi_yying@yahoo.com.cn

Xue-Shen Liu

Institute of Atomic and Molecular Physics, Jilin University, Changchun 130012, People's Republic of China

Xiao-Yan Liu

Institute of Atomic and Molecular Physics, Jilin University, Changchun 130012, People's Republic of China
Department of Mathematics, Northeast Normal University, Changchun 130024, People's Republic of China

Pei-Zhu Ding

Institute of Atomic and Molecular Physics, Jilin University, Changchun 130012, People's Republic of China

Received 12 May 2005; revised 6 June 2005

In this paper the asymptotic boundary condition (ABC) of 1-D model atom in the intense laser field at the spatial sufficiently far distance is presented using Fourier transformation on the condition that the initial state is local and the atomic potential in the model falls off rapidly. On the basis of this ABC, the symplectic algorithm is developed for computing the model atom in the intense laser field. The ABC and symplectic algorithm are applied to compute the ionization behaviors for 1-D Pöschl–Teller short-range potential. The numerical results illustrate that the ABC and the symplectic algorithm presented are reasonable and effective for 1-D model atom in the intense laser field.

KEY WORDS: asymptotic boundary condition, symplectic algorithm, 1-D Pöschl–Teller short-range potential, ionization probability

*Corresponding author.

1. Introduction

With the rapid development of the laser technique, the theoretical research on the interaction between the intense laser and matter, such as the explanation for the new experimental phenomena, the prediction for the behavior and the law of the matter in the stronger laser field that are not realized in the lab and etc, are attractive [1]. The research on the interaction between the intense laser and atom includes both the electron emission in the laser field (for example, the multiphoton ionization [2], the tunneling ionization [3] and so on) and the photon emission (for example, the high harmonic generation [4]).

When the intensity of the laser field reaches up to $10^{13}\,\mathrm{Wcm}^{-2}$, the traditional perturbative theory in quantum mechanics will be invalidated for the interaction between the laser and atom [5]. In the past decade, various nonperturbative methods have been developed and adopted, i.e., Floquet theory method [6], R-matrix method [7], etc, but these methods cannot be applied to the super-short and super-intense laser field. The methods solving directly numerically time-dependent Schrödinger equation (TDSE) have been applied to describe the interaction between the super-short and super-intense laser and atom, that is, TDSE is directly discretized using finite difference [8], discrete variable representation [9], finite elements [10], B splines [11] or a basis set expansion approach. In the basis set expansion approach, the basis function set may be chosen as the eigenstate of free-field [12,13], Volkov state [14] and so on.

When one of the finite difference method, the finite elements method and B splines function method is applied to solve numerically TDSE, it is necessary to truncate at the spatial sufficiently far distance and to choose the appropriate boundary condition. Because the laser field is stronger, the wave function at the spatial sufficiently far distance cannot be simply given as 0. In the previous literature, the various boundary conditions [15–17] have been developed and adopted on the basis of the theoretical analysis for the physical problem.

In this paper the asymptotic boundary condition (ABC) of 1-D model atom in the intense laser field at the spatial sufficiently far distance is presented using Fourier transformation under the condition that the initial state is local and the atomic potential falls off rapidly (Section 2). Using ABC the infinite spatial initial value problem of TDSE for 1-D model atom in the intense laser field is truncated into the finite spatial initial-boundary value problem, and this initial-boundary problem is numerically solved using the symplectic algorithm (Section 3), and thus the symplectic algorithm is extended from solving the time-independent problem [18–20] to solving the time-dependent problem. Then the ABC and the symplectic algorithm are applied to compute the ionization probability, the population probability of each bound states and continuum and the Rabi oscillation for 1-D model Pöschl–Teller (P–T) potential in the intense laser field (Section 4). The results illustrate that the ABC and the symplectic algorithm

presented are reasonable and effective for 1-D model atom in the intense laser field.

2. Asymptotic boundary conditions

In the length gauge and the electric-dipole approximation, the interaction between 1-D model atom and the intense laser field is described by the initial value problem of TDSE (we will use atomic units hereafter unless it is mentioned specifically)

$$i\frac{\partial}{\partial t}\psi(x,t) = \left[-\frac{1}{2}\frac{\partial^2}{\partial x^2} + V_0(x) + \varepsilon(t)x\right]\psi(x,t), \quad (-\infty < x < \infty, 0 \leqslant t \leqslant T) \tag{1}$$

$$\int_{-\infty}^{\infty} |\psi(x,t)|^2 \,\mathrm{d}x = 1, \quad (0 \leqslant t \leqslant T) \tag{2}$$

$$\psi(x,0) = \varphi(x)\int_{-\infty}^{\infty} |\varphi(x)|^2 \,\mathrm{d}x = 1, \quad (-\infty < x < \infty) \tag{3}$$

where the laser field is linearly polarized, and $\varepsilon(t)x = f(t)\varepsilon_0 x\sin(\omega_0 t)$ is the interaction between the laser and atom, where ε_0 is the peak amplitude of the laser field, $f(t)$ is the pulse-shape, T is the pulse width and ω_0 is the frequency of the laser field. The initial state $\varphi(x)$ is local, the atomic potential $V_0(x)$ is local or falls off rapidly, that is to say, for a sufficiently large parameter $X_0 > 0$, when $|x| > X_0$, $\varphi(x) = 0$ and $V_0(x) = 0$ or $|V_0(x)| \ll |\varepsilon_0 x|$. Because the interaction between laser and atom is greater than the atomic potential $|\varepsilon_0 x| \gg |V_0(x)|$ at the spatial sufficiently far distance, the atomic potential $V_0(x)$ can be neglected in the equation (1). When x is sufficiently large, the solution $\psi^w(x,t)$ of TDSE

$$i\frac{\partial}{\partial t}\tilde{\psi}(x,t) = \left[-\frac{1}{2}\frac{\partial^2}{\partial x^2} + \varepsilon(t)x\right]\tilde{\psi}(x,t) \quad (-\infty < x < \infty, 0 \leqslant t \leqslant T) \tag{4}$$

satisfies the conditions (2) and (3), and it is asymptotic to the solution of the initial value problem (1)–(3), thus it, called the *ABCs*, can be taken as the boundary condition of 1-D model atom in the intense laser field at the spatial sufficiently far distance $x \geqslant R$, where R is the boundary satisfying the physical meaning and $R > X_0 > 0$. By Fourier transformation and simplification, the initial value problem (3) and (4) is transformed into

$$i\frac{\partial\hat{\tilde{\psi}}(\omega(t),t)}{\partial t} - i\varepsilon(t)\frac{\partial\hat{\tilde{\psi}}(\omega(t),t)}{\partial\omega(t)} = \frac{1}{2}\omega^2\hat{\tilde{\psi}}(\omega(t),t), \tag{5}$$

$$\hat{\tilde{\psi}}(0, \omega(0)) = \hat{\varphi}(\omega(0)), \tag{6}$$

where $\hat{\tilde{\psi}} = F[\tilde{\psi}]$ is the Fourier transformation of $\tilde{\psi}(x, t)$, $\omega(t)$ is a formal variable during the Fourier transformation and $\omega(0)$ is the initial value of $\omega(t)$. The solution $\hat{\tilde{\psi}}(\omega(t), t)$ of the initial value problem (5) and (6) can be easily solved by inverse Fourier transformation

$$\psi^w(x, t) = \frac{1-i}{2\sqrt{\pi t}} \exp\left(iA(t)x - \frac{i}{2}q(t)\right) \int_{-\infty}^{\infty} \varphi(x') \exp\left(\frac{i(x-\alpha(t)-x')^2}{2t}\right) \mathrm{d}x' \tag{7}$$

which is just the wave function of the free electron in the laser field (Volkov wave function) [21], where $A(t) = -\int_0^t \varepsilon(t')\mathrm{d}t'$, $A(0) = 0$; $q(t) = \int_0^t A^2(t')\mathrm{d}t'$, $\alpha(t) = -\int_0^t A(t')\,\mathrm{d}t'$. When $|x| > X_0$, $\varphi(x) = 0$, then

$$\psi^w(x, t) = \frac{1-i}{2\sqrt{\pi t}} \exp\left(iA(t)x - \frac{i}{2}q(t)\right) \int_{-X_0}^{X_0} \varphi(x') \exp\left(\frac{i(x-\alpha(t)-x')^2}{2t}\right) \mathrm{d}x' \tag{8}$$

is the ABC of 1-D model atom in the laser field at the spatial sufficiently far distance x,

$$\psi(x, t) = \psi^w(x, t) \quad (|x| > X_0). \tag{9}$$

Furthermore, when $x > X_0$, the integrated function of the formula (8) vibrates drastically, and the value of the formula (9) is obtained using the numerical integrated method for the drastically vibration function. From the calculation results, we find that the integrated value is small but not zero, as has an important physical meaning and is a warrant of zero boundaries. We may assure the small distance of the zero boundaries from (9). We don't adopt the zero boundaries but ABC in our calculation for the sake of the numerical precise.

3. Symplectic algorithm for 1-D model atom in the intense laser field

When the infinite space $(-\infty, \infty)$ is truncated into the finite space $[-R, R]$ using the formula (9), the initial value problem (1)–(3) in the infinite space is transformed into the initial-boundary value problem in the finite space

$$i\tfrac{\partial}{\partial t}\psi(x, t) = \left[-\tfrac{1}{2}\tfrac{\partial^2}{\partial x^2} + V_0(x) + \varepsilon(t)x\right]\psi(x, t), \quad (-R \leqslant x \leqslant R, 0 \leqslant t \leqslant T), \tag{1'}$$

$$\psi(x, t) = \psi^w(x, t) \quad (|x| \geqslant R, 0 < t \leqslant T), \tag{2'}$$

$$\psi(x, 0) = \varphi(x) \quad \int_{-R}^{R} |\varphi(x)dx| = 1 \quad (-R \leqslant x \leqslant R). \tag{3'}$$

Let $\psi(x,t) = a(x,t) + ib(x,t)$ and $V(x,t) = V_0(x) + \varepsilon(t)x$. For a sufficiently large natural number N and the spatial step $h = R/N$, $x_j = jh$, $j = -(N+1), -N, \ldots, -1, 0, 1, \ldots, N, (N+1)$ denotes the spatial discrete node. From the formula (9), we have

$$\begin{aligned} &\psi^w(-x_{-N-1},t) = a_{-N-1}(t) + ib_{-N-1}(t), \quad && \psi^w(x_{N+1},t) = a_{N+1}(t) + ib_{N+1}(t) \\ &\psi^w(-x_{-N},t) = a_{-N}(t) + ib_{-N}(t), && \psi^w(x_N,t) = a_N(t) + ib_N(t) \end{aligned} \tag{10}$$

The spatial partial derivative $\partial^2/\partial x^2 \psi(x_j,t)$ of TDSE (1′) is substituted by the central differential $\partial^2\psi_j/\partial x_j^2 = -(\psi_{j-2} - 16\psi_{j-1} + 30\psi_j - 16\psi_{j+1} + \psi_{j+2})/(12h^2)$, the equation (1′) and the boundary conditions (2′) are discretized into the canonical equation

$$\begin{cases} \dot{A} = SB + Y_2, \\ \dot{B} = -SA - Y_1, \end{cases} \tag{11}$$

where $A = (a_{-N+1}, \ldots, a_{N-1})^T$, $B = (b_{-N+1}, \ldots, b_{N-1})^T$, $Y_1 = \frac{1}{24h^2}\big(a_{-N-1} - 16a_{-N}, a_{-N}, 0, \ldots, 0, a_N, -16a_N + a_{N+1}\big)^T$, $Y_2 = \frac{1}{24h^2}(b_{-N-1} - 16b_{-N}, b_{-N}, 0, \ldots, 0, b_N, -16b_N + b_{N+1})^T$, where the superscript T denotes the matrix transpose, $S = U + V$,

$$U = \frac{1}{24h^2}\begin{bmatrix} 30 & -16 & 1 & & & & 0 \\ -16 & 30 & -16 & 1 & & & \\ 1 & -16 & 30 & -16 & 1 & & \\ & \ddots & \ddots & \ddots & \ddots & \ddots & \\ & & 1 & -16 & 30 & -16 & 1 \\ & & & 1 & -16 & 30 & -16 \\ 0 & & & & 1 & -16 & 30 \end{bmatrix},$$

$$V = \begin{bmatrix} V(x_{-N+1},t) & & 0 \\ & \ddots & \\ 0 & & V(x_{N-1},t) \end{bmatrix}.$$

Let $Z = (A^T, B^T)^T$, $Y = (Y_1^T, Y_2^T)^T$, the canonical equation (11) can be rewritten as

$$\dot{Z} = GZ + JY = JCZ + JY. \tag{12}$$

It is obvious that S and $C = \begin{bmatrix} S & 0 \\ 0 & S \end{bmatrix}$ are both real symmetric matrixes, $J = \begin{bmatrix} 0 & I \\ -I & 0 \end{bmatrix}$

is the standard symplectic matrix, $G = \begin{bmatrix} 0 & S \\ -S & 0 \end{bmatrix} = JC$ is an infinitesimal symplectic matrix. Hamiltonian function of the system is

$$H(B, A, t) = \tfrac{1}{2}B^T SB + Y_2^T B + \tfrac{1}{2}A^T SA + Y_1^T A = H_1(B, t) + H_2(A, t) \quad (13)$$

This is a separable Hamiltonian system. Hence the canonical equation (11) or (12) can be numerically solved using the symplectic schemes of the separable Hamiltonian system, for example, the 4-stage fourth-order explicit symplectic schemes

$$\begin{array}{llll} \mu_1 = B^k - c_1\tau H_{1A}|_{t^k,A^k}, & \xi_1 = t^k + c_1\tau; & \nu_1 = A^k + d_1\tau H_{2B}|_{\xi_1,\mu_1}, & \zeta_1 = t^k + d_1\tau; \\ \mu_2 = \mu_1 - c_2\tau H_{1A}|_{\zeta_1,\nu_1}, & \xi_2 = \xi_1 + c_2\tau; & \nu_2 = \nu_1 + d_2\tau H_{2B}|_{\xi_2,\mu_2}, & \zeta_2 = \zeta_1 + d_2\tau; \\ \mu_3 = \mu_2 - c_3\tau H_{1A}|_{\zeta_2,\nu_2}, & \xi_3 = \xi_2 + c_3\tau; & \nu_3 = \nu_2 + d_3\tau H_{2B}|_{\xi_3,\mu_3}, & \zeta_3 = \zeta_2 + d_3\tau; \\ B^{k+1} = \mu_3 - c_4\tau H_{1A}|_{\zeta_3,\nu_3}, & \xi_4 = \xi_3 + c_4\tau; & A^{k+1} = \nu_3 + d_4\tau H_{2B}|_{\xi_4,B^{k+1}}, & \zeta_4 = \zeta_3 + d_4\tau. \end{array} \quad (14)$$

where the H_{1A} and H_{2B} are the partial derivation for A and B, respectively, and $\alpha=(2-2^{1/3})^{-1}$, $\beta=1-2\alpha$; $c_1=0$, $c_2=\alpha$, $c_3=\beta$, $c_4=c_2$, $d_1=\alpha/2$, $d_2=(\alpha+\beta)/2$, $d_3=d_2$, $d_4=d_1$ [22].

The above procedure is called the symplectic algorithm of computing 1-D model atom in the intense field, i.e., the initial value problem in the infinite space for 1-D TDSE in the intense field is transformed into the initial-boundary value problem in the finite space using ABC, and this initial-boundary problem is discretized into the canonical equation for a separable Hamiltonian substituting the central differential for the spatial partial derivation, and this Hamiltonian canonical equation can be numerically solved using the symplectic schemes for the separable Hamilton system.

4. Numerical results

The ionization behaviors of 1-D P–T short-range potential [15, 16]

$$V_0(x) = -\frac{U_0}{\cosh^2(\alpha_0 x)} \quad (15)$$

can be evaluated in the intense laser field. The P–T potential possesses the following properties,

1. $V_0(x)$ is an even function, namely, $V_0(-x) = V_0(x)$.
2. $|V_0(x)|$ falls off exponentially with increasing $|x|$.
3. There is a finite number of bound levels for given parameters U_0 and α_0.

4.1. Ionization behavior for the P–T potential with one bound state

To validate that the ABC and the symplectic algorithm presented in this paper are reasonable and effective for the interaction between the laser and

atom, the same parameters are chosen as the reference [15,16]. For $U_0 = 1$ and $\alpha_0 = 1$, there is only one bound state with eigenenergy $E_0 = -0.5$ a.u. for the P–T potential, and the corresponding normalized eigenfunction $\varphi_o(x) = 1/\sqrt{2}\text{coshx}$, which is chosen as the initial state. The laser field

$$\varepsilon(t)x = \varepsilon_0 x \sin(\omega_0 t). \tag{16}$$

is linear polarized.

In this calculation, the frequency $\omega_0 = 0.2$ a.u., the spatial step $h = 0.1$ a.u. and the temporal step $\tau = 0.001$ a.u. are chosen. The wave function in the range [−50 a.u., 50 a.u.] and the wave function's norm with the time are represented in figure 1 when the laser intensity $\varepsilon_0 = 0.1$ a.u., the boundary is imposed on 600 a.u. and the time is after 16 optical periods pulse. The ionization probability of the electron

$$P_{\text{ion}} = 1 - P_{\text{b}} \tag{17}$$

is computed with the laser intensity for the P–T potential in the laser field for the frequency $\omega_0 = 0.2$ a.u. and the boundary 600 a.u. The results are given in figure 2, where P_{b} is the total population of all the bound states. The probability density of the electronic wave function

$$P(x, T) = |\psi(x, T)|^2 \tag{18}$$

is evaluated and shown in figure 3.

Figure 1(a) is identical to figure 2 in the ref. [15], which shows that the ABC presented in this paper is reasonable and precise for the interaction between the laser and atom. The difference of the absolute value of the wave functions between the boundaries imposed on 600 a.u. and 700 a.u. is shown in figure 1(b), whose maximum is within the numerical computing error 10^{-4}. In figure 1(c), the wave function's norm with the time is greater than 1 at a few points but does not exceed 10^{-11}, which is far less than the numerical error 10^{-4}, and less than 1 at the most points. This result shows that there are some probabilities for electrons to be ionized into the free electron and they cannot be recombined to the parent atom.

The ionization curve in figure 2 is identical to figure 6 in the ref. [15] and figure 3 in the ref. [16], which further shows that the ABC presented in this paper is reasonable and precise and the symplectic algorithm is steady for the interaction between the laser and atom. The extrema points on the ionization curves correspond to the suppression of 3-photon ionization (A) and 4-photon ionization (B), respectively, the reason is that when

$$n\omega_0 < |E_0| + U_{\text{p}}, \quad U_{\text{p}} = \varepsilon_0^2/4\omega_0^2, \tag{19}$$

n-photon ionization is suppressed. Furthermore, it is seen that the ionization curves are similar for the different pulse width, but the ionization amplitude

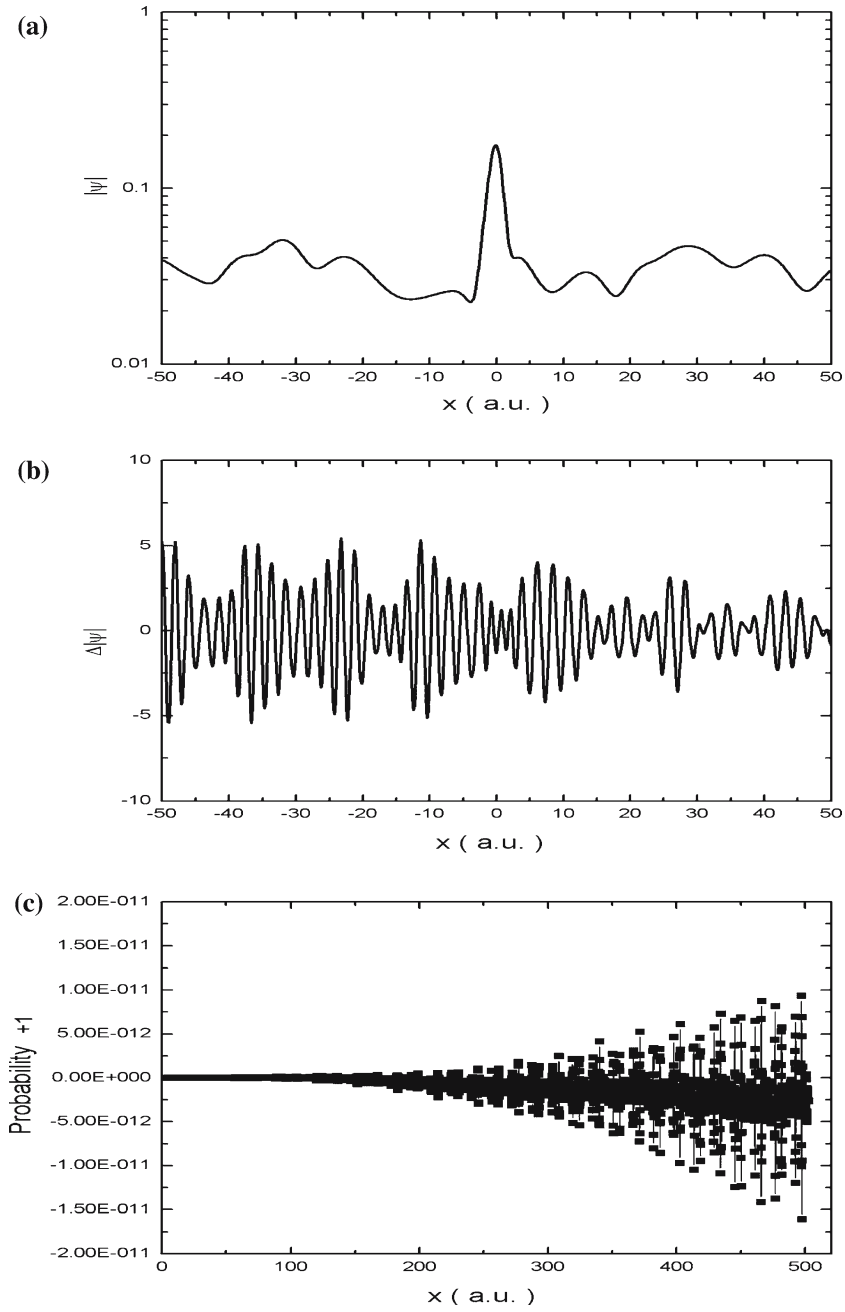

Figure 1. (a) Numerical solution $|\psi(x)|$ after 16 light periods for $\varepsilon_0 = 0.1$ a.u. and $\omega_0 = 0.2$ a.u., (b) Relative difference in units of 10^{-5}between the truncated solutions with boundaries at $x = \pm 600$ a.u. and $x = \pm 700$ a.u. and (c) the wave function's norm for $x = \pm 700$ a.u.

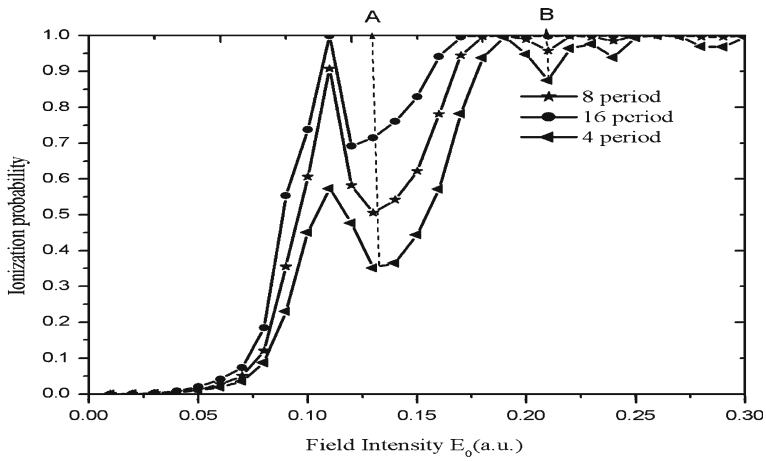

Figure 2. The ionization probability with the laser peak intensity after four (◄), eight (★) and sixteen (●) light periods for the monochromatic with frequency $\omega_0 = 0.2$ a.u.

is only different. The longer the laser pulse width is, the larger the ionization amplitude is. From figure 3, the wave function spreads outside both boundaries with increasing the laser intensity. The stronger the laser intensity is, the more widely the wave function spreads.

Our results show that the ABC and the symplectic algorithm presented in this paper are reasonable and effective for the interaction between the laser and atom, and the ABC is simpler than the previous boundary conditions in considering the physical idea and the mathematical deduced procedure. In next section, the ionization behaviors of the electron in P–T potential with three bound states in the laser field are computed, which is more interesting and more meaningful.

4.2. *P–T potential with three bound states*

The P–T potential for the parameters $U_0 = 0.7, \alpha_0 = 0.4$

$$V_0(x) = -\frac{0.7}{\cosh^2(0.4x)} \tag{20}$$

possesses the three bound states, whose eigenenergies and corresponding normalized eigenfunctions are,

$$E_0 = -0.5\,\text{a.u.}, \quad E_1 = -0.18\,\text{a.u.},$$
$$E_2 = -0.02\,\text{a.u.}, \quad \varphi_0(x) = \frac{4}{\sqrt{15\pi}}(\cosh(\alpha_0 x))^{-2.5},$$
$$\varphi_1(x) = \frac{4}{\sqrt{5\pi}}(\cosh(\alpha_0 x))^{-1.5}\tanh(\alpha_0 x),$$

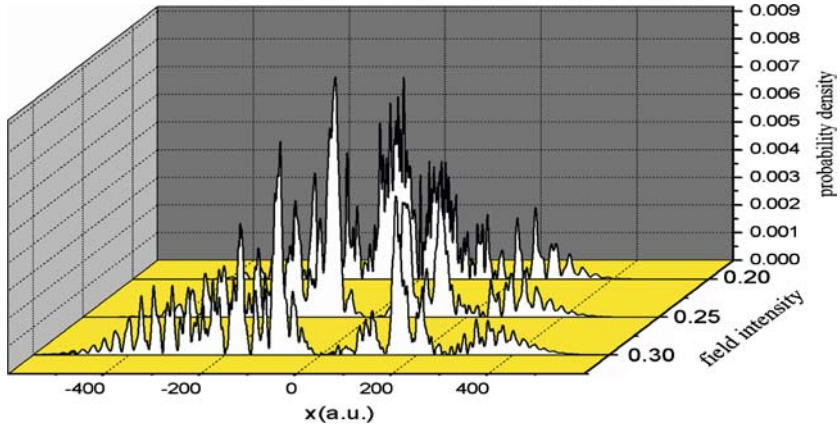

Figure 3. Probability density of wave function with the peak value of the laser intensity.

$$\varphi_2(x) = \sqrt{\frac{6}{5\pi}}\left[(\cosh(\alpha_0 x))^{-0.5} - \frac{4}{3}(\cosh(\alpha_0 x))^{-2.5}\right],$$

respectively. The ionization behaviors of the P–T potential are computed in the laser fields

$$\varepsilon(t) = \begin{cases} \varepsilon_0 \sin(\omega_0 t) & (t_{\text{on}} \leqslant t \leqslant NT_0), \\ 0 & (NT_0 \leqslant t \leqslant t_{\text{off}}), \end{cases} \tag{21}$$

and

$$\varepsilon(t) = \begin{cases} \varepsilon_0 \sin^2\left(\frac{\omega_0 t}{2N}\right) \sin(\omega_0 t) & (t_{\text{on}} \leqslant t \leqslant NT_0), \\ 0 & (NT_0 \leqslant t \leqslant t_{\text{off}}), \end{cases} \tag{22}$$

respectively, where $T_0 = 2\pi/\omega_0$ is the optical period of the laser field. In the following calculation, 15 optical periods are chosen as the pulse width, the ground state $\varphi_0(x)$ of the P–T potential (20) as the initial state, and the laser frequency is chosen as the Rabi oscillation frequency between the ground state and the first excited state, which is $\omega_0 = 0.32$ a.u.

(1) *Rabi oscillation between the ground state and the first excited state*

When the laser intensity is weaker, the Rabi oscillation between the ground state and the first excited state will be the dominant process, and the transition rate between these energy levels will speed with the increase of the laser intensity, which is shown in figure 4. This result is identical to that of the perturbative theory in the traditional quantum mechanics. The oscillation depends strongly on the pulse-shape, and is suppressed faster for the rectangle pulse-shape than for the approximate gauss pulse-shape with the increase of the laser intensity.

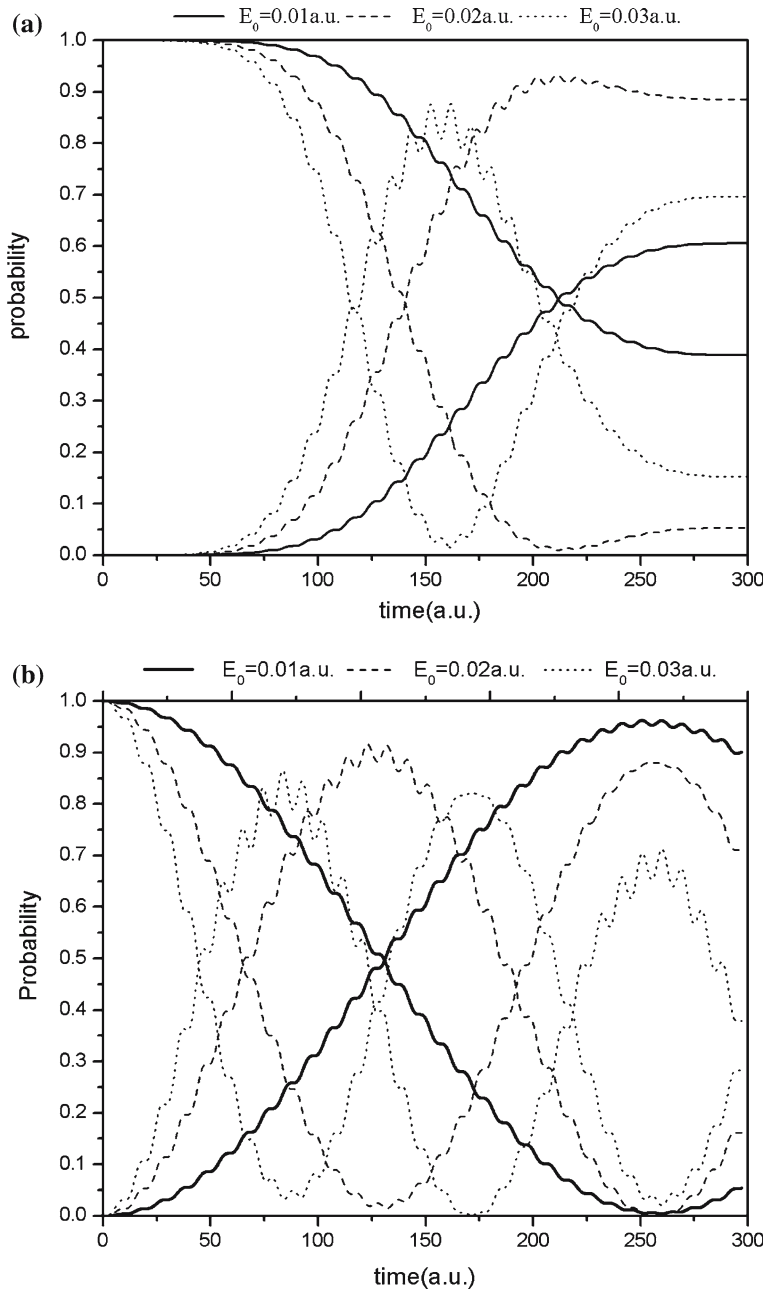

Figure 4. Rabi association (a) Irradiated by the approximate gauss pulse (b) Irradiated by the rectangle pulse.

(2) *Population probability of each state with the laser intensity for the different pulse-shape*

With the increase of the laser intensity, the effect of Rabi oscillation is weakened gradually and the ionization is strengthened, hence the electron reaches directly to the ionized continuum state by multi-photon ionization or tunneling ionization as well as over-barrier ionization. The population probability of each bound state

$$P_i(t) = |\langle \varphi_i(x)|\psi(x,t)\rangle|^2 \tag{23}$$

changes with the laser intensity for both the rectangle pulse-shape and the approximate gauss pulse-shape, shown in figure 5, which illustrates that the population probability of the bound states depends obviously on the pulse-shape. The probability of the electron recombination is greater for the approximate gauss pulse-shape than the rectangle pulse-shape, and the population of the bound electron is greater for the approximate gauss pulse-shape than the rectangle pulse at the end of the laser pulse-shape at the time after the pulse.

The population probability of the continuum state is

$$P_c(t) = 1 - \sum_i P_i(t), \tag{24}$$

where the summation is over all the bound states and the result is also exhibited in figure 5. From the figure we can see that the ionization is strengthened with the increase of the laser intensity. Especially, when the laser intensity reaches up to the critical intensity of 0.0625 a.u. [12], the electron can freely go through the potential barrier and be ionized, which is called the over-barrier ionization. When the laser intensity is greater than this value, the population of the continuum will be greater than that of the bound states, and thus the ionization will be the dominant process.

(3) *Ionization probability with the laser intensity for the different pulse-shape*

The ionization probability is

$$P_{\text{ion}}(t) = 1 - \sum_i^n P_i(t) = 1 - \sum_i^n |\langle \varphi_i(x)|\psi(x,t)\rangle|^2. \tag{25}$$

Figure 6 shows that the ionization probability changes with the time and the laser intensity for the two different pulse-shapes, 6(a) the approximate gauss pulse-shape and 6(b) the rectangle pulse-shape. Figure 6(c) is the curve of the ionization probability in the laser field at the time after the pulse. The figures illustrate that the ionization probability depends on the laser pulse-shape, but the total ionization trend is similar and the ionization amplitude is different for the different pulse-shape.

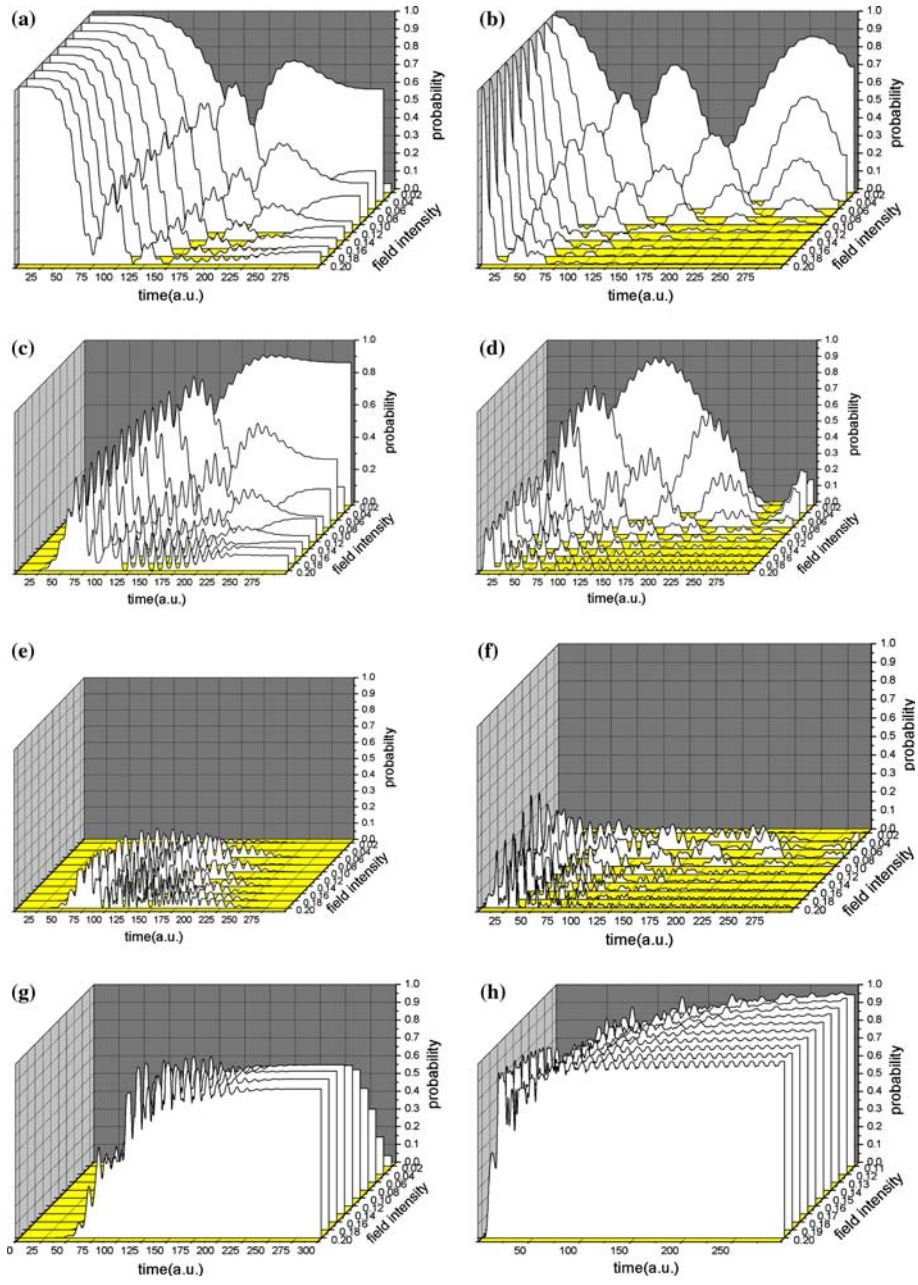

Figure 5. Population of the ground state, the first excited state, the second excited state and the ionization continuum in the laser field for the different laser pulse-shape: (a), (c), (e), (g) Irradiated by the approximate gauss pulse, (b), (d), (f), (h) Irradiated by the rectangle pulse.

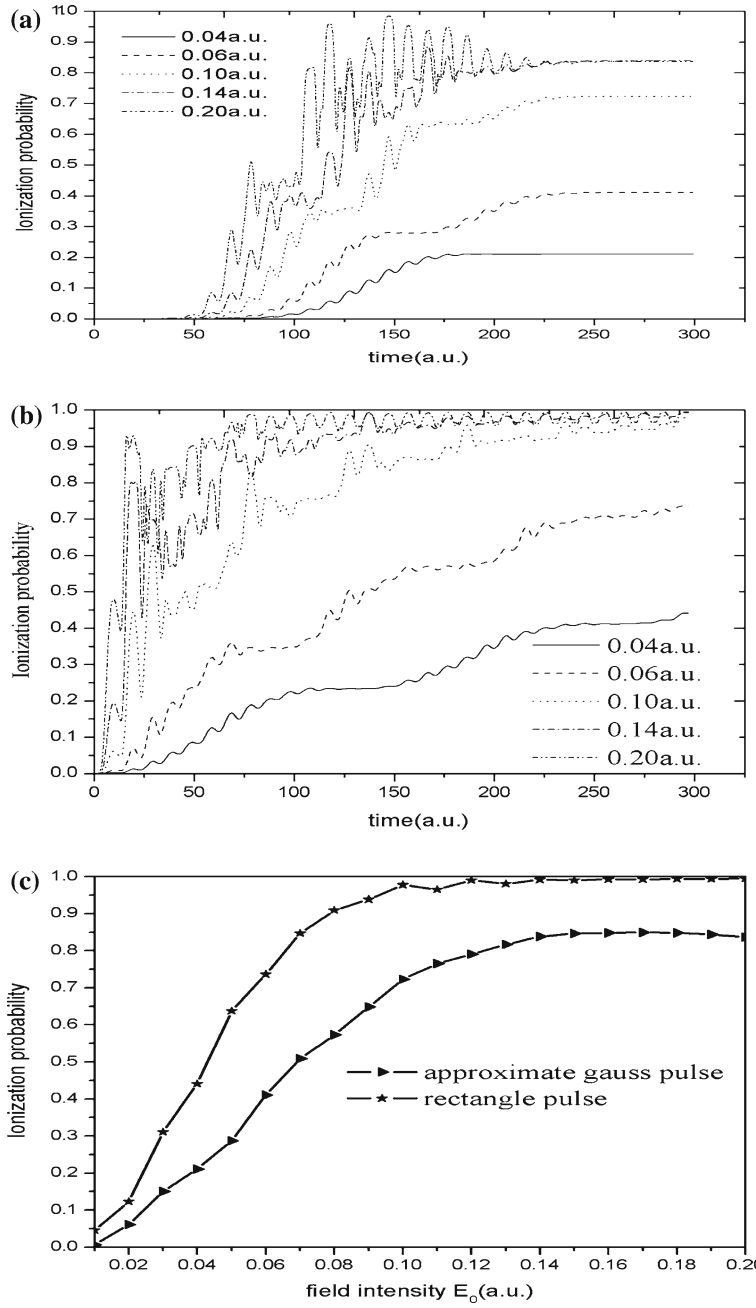

Figure 6. The ionization probability in the laser field: (a) Irradiated by the approximate gauss pulse, (b) Irradiated by the rectangle pulse.

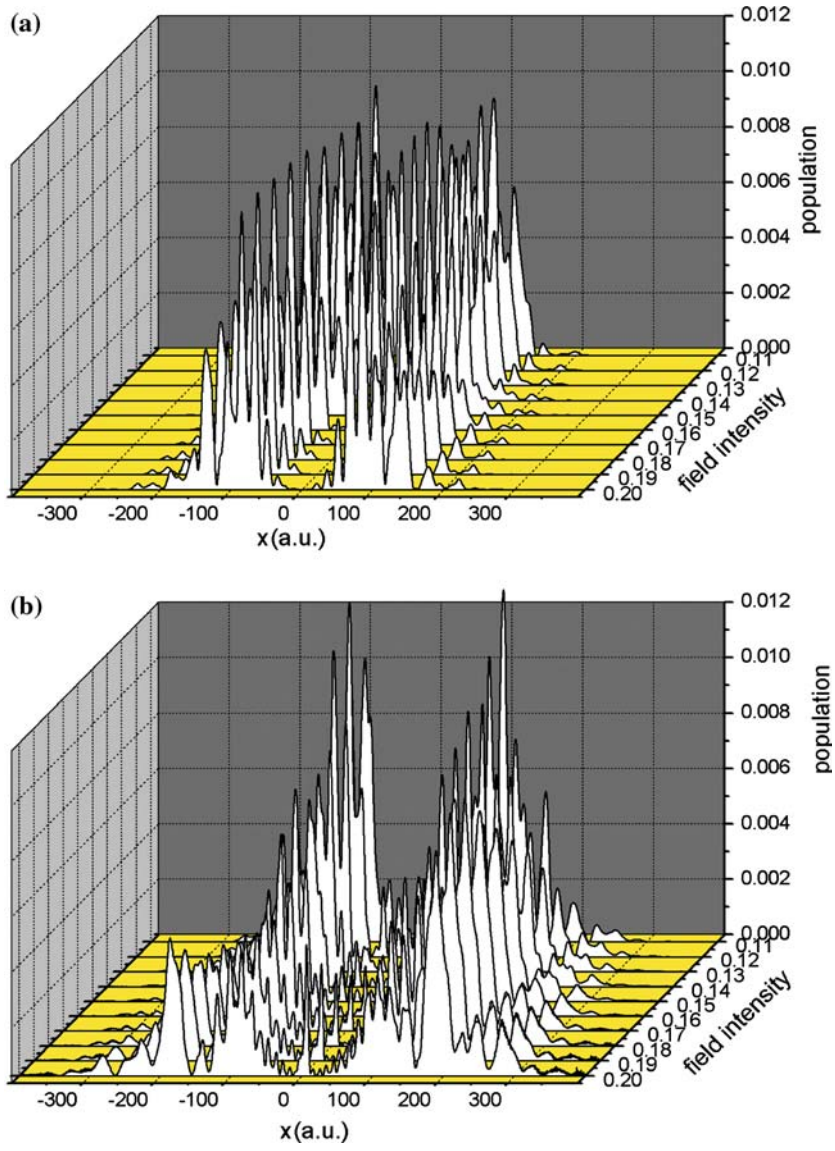

Figure 7. Population of the ionization continuum state: (a) Irradiated by the approximate gauss pulse, (b) Irradiated by the rectangle pulse.

(4) *Probability density of the ionization continuum state with the laser intensity*

The probability density of the continuum state is

$$\rho_{\mathrm{c}} = |\psi_c^*(x,t)\psi_c(x,t)|, \tag{26}$$

where $\psi_c(x,t) = \psi(x,t) - \sum_i \langle\varphi_i(x)|\psi(x,t)\rangle\varphi_i(x)$ is the wave function of the ionized continuum state and the summation is over all the bound states. The curve

of the probability density of the ionized continuum state in the laser field is displayed in figure 7, which illustrates that the spread of the electron is enhanced with the increase of the laser intensity in the space. The electron spreads more widely for the rectangle pulse-shape than the approximate gauss pulse-shape.

5. Conclusion

The ionization and the recombination of the electron induced by the laser field depends obviously on the laser pulse-shape, which is the reason why the different pulse-shape are adopted for the different physical problems. The rectangle pulse is adopted for the research on the ionization, because the electrons are ionized more for the rectangle pulse than the approximate gauss pulse. However, the approximate gauss pulse is adopted for the research on the high harmonic generation, because the high harmonic generation needs the electronic recombination process and the recombination probability is greater more for the approximation gauss pulse than the rectangle pulse.

The ABC and the symplectic algorithm presented in this paper are reasonable and effective for 1-D model atom in the intense laser field. The ABC is independent of the atomic potential function and fits various model potentials and its deduced procedure is simple and elementary.

Acknowledgments

Projects supported by the National Natural Science Foundation of China (10171039, 10074019), and by The Special Funds for Major State Basic Research Projects (G1999032804) and by the Research start Foundation of Jiaxing University (70504045).

References

[1] J.H. Liu, R.X. Li, Z.Z. Xu and J.R. Liu, Phys. Rev. A 63 (2001) 033809.
[2] K.C. Kulander, Phys. Rev. Lett. 38 (1988) 778.
[3] L.V. Keldysh, JETP 47 (1964) 1945v (Sov. Phys. JETP 20 (1965) 1307).
[4] C. Lyngå, A. L'Huillier, C.-G. Wahlström, J. Phys. B 29 (1996) 3293.
[5] M. Nayfeh, *Atoms in Strong Fields* (Spring-Verlag, Berlin, 1990).
[6] R.M. Potvliege and Robin Shakeshaft, Phys. Rev. A 38 (1988) 4597.
[7] P.G. Burke, P. Francken and C.J. Joachain, J. Phys. B 24 (1991) 751.
[8] Q. Su, J.H. Eberly and J. Javanainen, Phys. Rev. Lett. 64 (1990) 862.
[9] B.I. Schneider, Phys. Rev. A 55 (1997) 3417.
[10] M. Gavrila and J. Shertzer, Phys. Rev. A 53 (1996) 3431.
[11] Jian Zhang and P. Lambropoulos, Phys. Rev. Lett. 77 (1996) 2186.
[12] S. Geltman, J. Phys. B 33 (2000) 1967.
[13] G.L. Kamta, T. Grisges, B. Piraux, R. Hasbani, E. Cormier and H. Bachau, J. Phys. B 34 (2001) 857.

[14] L.A. Collins and A.L. Merts, J. Opt. Soc. Am. B 7 (1990) 647.
[15] A.M. Ermolaev, I.V. Puzynin, A.V. Selin and S.I. Vinitsky, Phys. Rev. A 60 (1999) 4831.
[16] K. Boucke, H. Schmitz and H.-J. Kull, Phys. Rev. A 56 (1997) 763.
[17] E.Y. Sidky and B.D. Esry, Phys. Rev. Lett. 85 (2000) 5086.
[18] X.S. Liu, X.Y. Liu, Z.Y. Zhou, P.Z. Ding and S.F. Pan, Intern. J. Quant. Chem. 79 (2000) 343.
[19] X.S. Liu, L.W. Su, X.Y. Liu and P.Z. Ding, Intern. J. Quant. Chem. 83 (2001) 303.
[20] X.S. Liu, L.W. Su and P.Z. Ding, Intern. J. Quant. Chem. 87 (2002) 1.
[21] L. Rosenberg and F. Zhou, Phys. Rev. A 47 (1993) 2146.
[22] S.K. Gray, D.E. Manolopoulos, J. Chem. Phys 104(18) (1996) 7099.